

This is a postprint version of the following published document:

Muñoz-Noval, Á., Salas-Colera, E., & Ranchal, R. (2019). Local and medium range order influence on the magnetic behavior of sputtered Ga-rich FEGA thin films. *Journal of Physical Chemistry C*, 123(20), 13131-13135.

DOI: [10.1021/acs.jpcc.9b01889](https://doi.org/10.1021/acs.jpcc.9b01889)

© 2019 American Chemical Society

# Local and Medium Range Order Influence on the Magnetic Behavior of Sputtered Ga-Rich FeGa Thin Films

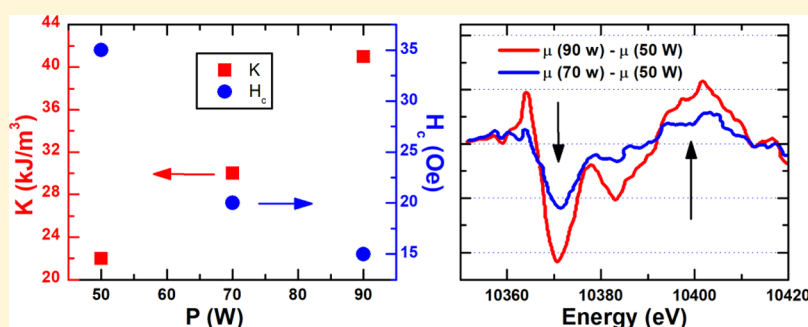
A. Muñoz-Noval,<sup>†,‡</sup> E. Salas-Colera,<sup>\*,§,||</sup> and R. Ranchal<sup>‡</sup>

<sup>†</sup>Department of Applied Chemistry, Hiroshima University, Higashi-Hiroshima, Hiroshima 739-8527, Japan

<sup>‡</sup>Departamento de Física de Materiales, Facultad de Ciencias Físicas, Universidad Complutense de Madrid, Ciudad Universitaria s/n, Madrid 28040, Spain

<sup>§</sup>BM25-Spline, The Spanish CRG at the ESRF, Grenoble 38043, France

<sup>||</sup>Instituto de Ciencia de Materiales de Madrid-CSIC, Madrid 28049, Spain



**ABSTRACT:** We have investigated the influence of the growth power on the structural properties of Fe<sub>100-x</sub>Ga<sub>x</sub> ( $x$  ca. 29) films sputtered in the ballistic regime in the oblique incidence. By means of different structural characterizations, mainly X-ray diffraction and X-ray absorption spectroscopy, we have reached a deeper understanding about the influence of the local and medium range order on the magnetic behavior of Ga-rich FeGa thin films. On the one hand, the increase of the growth power reduces the crystallite size (medium order) that promotes the decrease of the coercive field of the layers. On the other hand, the growth power also determines the local order as it controls the formation of the A2, B2, and D0<sub>3</sub> structural phases. The increase of the uniaxial in-plane magnetic anisotropy with growth power has been correlated with the enhancement of both Ga pairs and a tetragonal distortion. The results presented in this work give more evidence about the magnetic anisotropy sources in Ga-rich FeGa alloys, and therefore, it helps to understand how to achieve a better control of the magnetic properties in this family of alloys.

## INTRODUCTION

Fe<sub>100-x</sub>Ga<sub>x</sub> compounds are among the most relevant magnetostrictive materials with excellent ductility, chemical stability, and free of rare-earths. Their magnetostriction coefficient ( $\lambda_s$ ) depends on the Ga content and on the samples processing, showing two maxima around 18 and 28 at. % Ga being possible to enhance  $\lambda_s$  by means of fast cooling.<sup>1</sup> The highest  $\lambda_s$  value is achieved in quenched samples at the second maxima (Ga-rich FeGa alloys) of the Ga-dependent magnetostriction curve,<sup>1</sup> although up-to-date, major part of the research has been focused on the relationship between the microstructural, magnetic, and magnetoelastic properties at the first peak.<sup>2–14</sup> Less has been reported on Fe<sub>100-x</sub>Ga<sub>x</sub> alloys with compositions around the second maxima, in spite of their intrinsic interest.<sup>1,15–20</sup> The metastable diagram phase predicts an A2 single phase state just for Ga contents up to 21 at. %.<sup>1</sup> It is precisely when this A2 single phase state is obtained by means of quenching when the magnetostriction reaches its highest value in the first maximum of magnetostriction. The magnetostriction in the second peak is also larger when

quenching, but in general it exhibits an A2, B2, and D0<sub>3</sub> phase mixture.<sup>1,15</sup> Therefore, the origin of this second magnetostriction maximum seems to involve more factors than the first one. Because magnetostriction and magnetic anisotropy are closely related, investigations about the latter are crucial to understand the former.

Recently, the correlation between microstructure and the development of an in-plane magnetic anisotropy in Ga-rich FeGa alloys around the second peak has been reported.<sup>19,20</sup> In particular, the local range order promoted by the use of different sputtering regimes, ballistic or diffusive, was reported in a previous work.<sup>19</sup> To study the local range order, the use of X-ray absorption fine structure (XAFS) measurements is crucial because they can provide information about the electronic structure and local geometry of the scattering atom when using X-ray absorption near edge structure

Received: February 27, 2019

Revised: April 20, 2019

Published: April 29, 2019

(XANES) and about the degree of disorder by means of extended XAFS (EXAFS).<sup>9,19–22</sup> In the sputtering process, neutrals (atoms ejected from the target upon the impact of energetic particles) suffer collisions on their movement from the target to the substrate.<sup>23–25</sup> If the number of collisions is low, neutrals keep their momentum and energy till the substrate, and the sputtering growth takes place under ballistic flow.<sup>23</sup> In this regime, sputtered atoms arrive to the substrate with the same energy and momentum they acquired in the target. The ballistic flow regime increased the amount of ordered phases with respect to the diffusive, while the direction of the uniaxial magnetic easy axis seems to be set by the oblique incidence.<sup>20,26</sup> Actually, Zhang and co-workers have recently reported its use for controlling the magnetic anisotropy in exchange-biased InMn/FeGa bilayers.<sup>27</sup> Another key parameter in the sputtering technique is the growth power, tightly related to the growth rate that influences the microstructure and morphology of films at different scales.<sup>28–31</sup>

In this work, we address the influence of the growth power on Ga-rich FeGa thin films sputtered in the ballistic regime, in which we have observed that it is possible to fix the Ga content within a very narrow range. This allows us to better correlate the microstructure (medium and local range) promoted during sputtering growth with the magnetic properties of the layers. Thanks to this investigation, it has obtained a deeper understanding about the magnetic anisotropy origin in Ga-rich FeGa thin films and how to control it.

## METHODS

Samples were grown by the direct current (dc) magnetron sputtering technique at room temperature on glass substrates. The deposition was carried out in oblique incidence with an angle of 25° between the vapor beam and the sample plane. The distance between the target and the substrate was 9 cm that corresponds to the ballistic regime for the growth conditions used in this work.<sup>19</sup> We have used films of Mo with a thickness of 20 nm as buffer and capping layers. Mo was deposited by dc sputtering with a power of 90 W in an Ar pressure of 0.3 Pa. The 200 nm-thick FeGa films were deposited from a target with a composition of Fe<sub>72</sub>Ga<sub>28</sub> with a diameter of 5 cm and a thickness of 2 mm. The thickness of the layers has been chosen in order to promote the existence of a clear in-plane magnetic anisotropy.<sup>20</sup> We have used an Ar pressure of 0.3 Pa in all cases, whereas the growth power ranged from 50 to 90 W. The target voltage was monitored during the layers growth being around 430 V in all cases. In order to avoid effects related to the target ageing, the samples were deposited consecutively. The structure of the samples is glass/Mo (20 nm)/FeGa (200 nm)/Mo (20 nm).

X-ray diffractometry (XRD) in the Bragg–Brentano configuration was performed in a Philips X'Pert MPD using the Cu K $\alpha$  wavelength (1.5406 Å). The composition of the samples was analyzed by means of the energy dispersive X-ray spectroscopy in a Leica 440 scanning electron microscope operated at 8 kV and 1.5 nA. The in-plane hysteresis loops were measured at room temperature in a vibrating sample magnetometer from LakeShore.

The XAFS measurements were performed at BM25-Spline in the ESRF, the European Synchrotron in Grenoble (France). Both the Fe and Ga K-edges (7112 and 10367 eV, respectively) were analyzed measuring at fluorescence yield mode. The EXAFS data were treated applying standard

procedures employing the Demeter package.<sup>32</sup> The fits were carried out in *r*-space using theoretical functions from FEFF8.4 code calculated from crystallographic standards.<sup>33,34</sup>

## RESULTS AND DISCUSSION

As can be observed in Table 1, the Ga content of the FeGa layers is almost independent on the growth power. In this

**Table 1.** Ga Content as Measured by EDS, Lattice Parameter (*a*), and Grain Size (*D*) Inferred from XRD, and Parameters Inferred from EXAFS: Global Expansion/Contraction Coefficient of the Shells Respect to the Tabulated Crystallographic Reference ( $\Delta R$ ), Debye–Waller Factor of the First Ga–Ga/Fe Shell ( $\sigma^2$ Ga–Ga1), and Debye–Waller Factor of the Second Ga–Ga/Fe Shell ( $\sigma^2$ Ga–Ga2) for Fe<sub>100–x</sub>Ga<sub>x</sub> Alloys Deposited in the Ballistic Regime at Different Growth Powers (*P*) in the Oblique Deposition

	<i>P</i> = 50 W	<i>P</i> = 70 W	<i>P</i> = 90 W
Ga (at. %)	28(1)	29(1)	30(1)
<i>a</i> (Å)	2.894(2)	2.897(2)	2.899(2)
<i>D</i> (Å)	140(5)	104(5)	82(5)
<i>H</i> <sub>C,hard axis</sub> (Oe)	35	20	15
<i>K</i> (J/m <sup>3</sup> )	2.2 × 10 <sup>4</sup>	3.0 × 10 <sup>4</sup>	4.1 × 10 <sup>4</sup>
$\Delta R$ (Å)	0.08(1)	0.08(1)	0.08(1)
$\sigma^2$ Ga–Ga1 (Å <sup>2</sup> )	0.0074(3)	0.0074 (3)	0.0073(3)
$\sigma^2$ Ga–Ga2 (Å <sup>2</sup> )	0.0233(20)	0.0235(20)	0.0230(20)

work, the Ga content is constrained between 28 and 30 at. % when power increases from 50 to 90 W. Considering the experimental error, we can assume that Ga content is fixed for the studied power range. All the layers exhibit similar X-ray diffraction patterns with a main peak related to the  $\alpha$ -Fe (110) reflection as obtained in previous works (Figure 1).<sup>19,20,35</sup> The

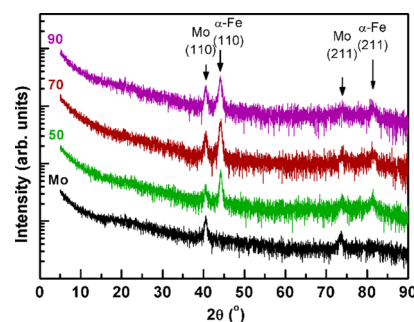


**Figure 1.** X-ray diffraction patterns in the Bragg–Brentano configuration for the FeGa films deposited in the ballistic regime at different growth powers: 90 W (90), 70 W (70), and 50 W (50). A Mo layer is included for further comparisons. The curves are vertically shifted for clarity.

lattice parameter (*a*) calculated using this (110) reflection slightly increases with the growth power, in agreement with the almost insignificant increase of the Ga content (Table 1). The Scherrer's equation (eq 1) using the  $\alpha$ -Fe(110) reflection has been employed to estimate the crystallite size (*D*). We have used this parameter *D* to characterize the medium range order

$$D = \frac{Q\lambda}{\beta \cos \theta} \quad (1)$$

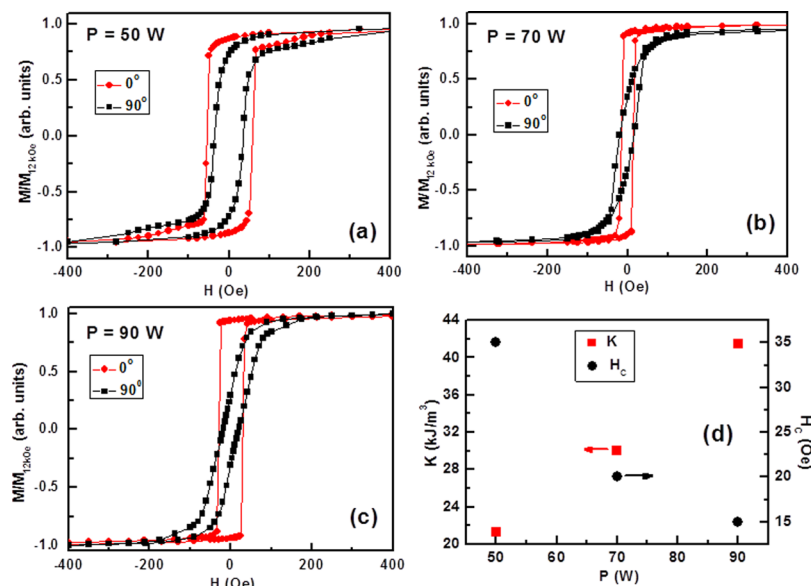


**Figure 2.** Hysteresis loops at room temperature measured in the sample plane for different directions between the reference direction and the applied magnetic field: (●) 0° and (■) 90° for FeGa films deposited in the ballistic regime at different growth powers: (a) 50, (b) 70, and (c) 90 W. (d) In-plane magnetic anisotropy ( $K$ ) and coercive field in the hard axis as a function of the growth power.

where  $Q$  is a shape factor taken as 0.9,  $\lambda$  is the radiation wavelength (1.5406 Å),  $\beta$  is the full width at half maximum, and  $\theta$  is the Bragg angle of the considered reflection, respectively. Here, we are assuming that variations on the full width at half maximum of the diffraction peak are only related to  $D$ . The observed decrease of the crystallite size with the growth power indicates a reduction of the medium range order (Table 1).

The growth power has also an influence on the magnetic behavior of the Ga-rich FeGa layers. In Figure 2a–c, we present the room temperature in-plane hysteresis loops with the applied magnetic field forming different angles with respect to the reference direction (sputtering incidence direction). A clear in-plane uniaxial magnetic anisotropy can be observed in all the considered samples, which is enhanced upon the increase of the growth power (Figure 2d). The easy axis coincides with the oblique incidence direction in agreement with previous works.<sup>19,26</sup> As it can also be observed in the set of magnetic loops, there is a decrease of the coercive field ( $H_C$ ) in the hard axis with the growth power (Figure 2d). We can understand this behavior by taking into account the dependence between the growth power and the crystallite size. It has been reported that magnetic domains with size below the magnetic coherence length ( $\delta$ ) present an increase of  $H_C$  with the grain size.<sup>36</sup>  $\delta$  can be calculated by means of eq 2

$$\delta = \sqrt{\frac{A}{K}} \quad (2)$$

where  $A$  is the exchange coupling constant and  $K$  the anisotropy energy of the FeGa layers. Taking into account  $A = 1.6 \times 10^{-11} \text{ J}\cdot\text{m}^{-1}$  and the experimental values for  $K$  (Table 1), we obtain a  $\delta$  of at least 19 nm. The highest estimated crystallite diameter determined by XRD data was 14 nm (see Table 1). Then, the smaller value of  $D$  in comparison to  $\delta$  can explain the coercivity diminishment with the growth power.

Up to this point, there seems to be a correlation between the coercivity and the medium range order originated by the growth power increase. If the grain size had any influence on

the magnetic anisotropy, it would be to decrease the anisotropy as generally observed in nanocrystalline systems due to the average of local fluctuating anisotropies.<sup>36</sup> Nevertheless, we have experimentally obtained the opposite behavior, that is, the magnetic anisotropy is higher in the layers with smaller grains. Therefore, the in-plane magnetic anisotropy must have another physical origin. In order to get a deeper insight into the structural properties of the layers, it is necessary to reach information about the local order because, in previous works, it has been reported to be closely related to the magnetic anisotropy.<sup>9,19–21</sup> Therefore, we have also tackled a more detailed study of the local structure of the layers by performing XAFS spectroscopy. The fitting of the EXAFS spectra performed in the  $r$ -space (Figure 3a) provides the structural parameters included in Table 1. The fittings of the short-range structure of Ga have been carried out considering a two atomic shell model in which the first shell is a Ga–Fe and the second a Ga–Ga shell. The structural parameters included in the model comprise a global expansion/contraction coefficient of the shells respect to the tabulated crystallographic reference ( $\Delta R$ ), the Debye–Waller factor ( $\sigma^2$ ), and the nonstructural parameter  $\Delta E_0$ , which accounts for the energy shifts of the theoretical calculated spectrum respect to the energy grid of the experimental one.<sup>37</sup> All the structural parameters are quite similar, being feasible to consider all of them equal within the experimental error (Table 1). The  $\Delta R$  parameter accounts for the shell distance dilatation respect to the tabulated value, and it is somehow related to the lattice parameter  $a$ . The fact that all the studied samples have approximately the same  $\Delta R$  value is compatible with the fact that the experimental lattice parameters are also similar for all the growth powers (Table 1). In the case of the  $\sigma^2$ , we can also assume that the static local disorder can be considered the same for all the layers. Therefore, in this study in which all the samples have a very close composition, EXAFS does not provide relevant information about differences between samples.

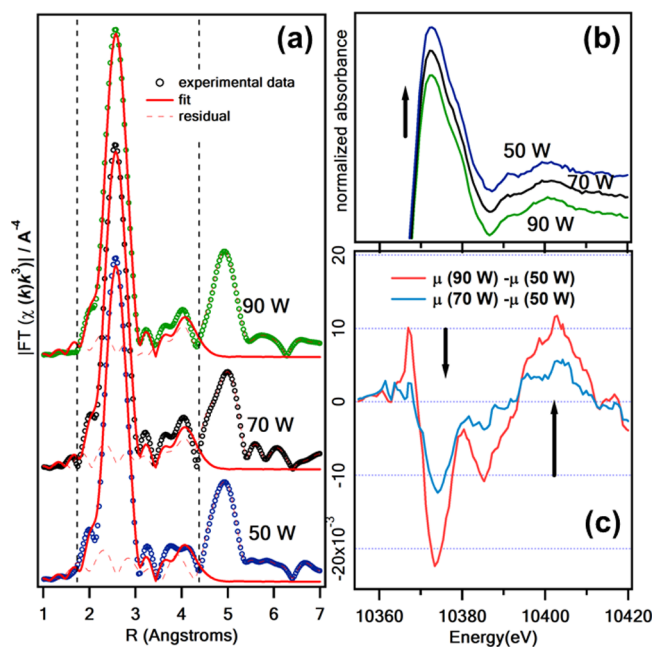


**Figure 3.** XAFS spectra of the FeGa layers grown by sputtering in the ballistic regime for increasing growth powers, 50, 70, and 90 W. (a) Fourier transform of the EXAFS spectra and best fits. (b) Detail of the main peak (white line) of the absorption edge in XANES for the different growth powers. (c) Subtracted spectra with respect to that for 50 W. For example,  $\mu(90\text{ W}) - \mu(50\text{ W})$  indicates the subtraction between the spectra for layers deposited at 90 and 50 W, respectively.

local range order can be tuned by means of the growth power when the Ga concentration is fixed in a very narrow range. In this study, the magnetic anisotropy is controlled by both, Ga-pairs and tetragonal distortion. A similar conclusion was obtained when studying the effect of the thickness.<sup>20</sup> Therefore, the correlation between magnetic anisotropy and both, Ga-pairs and tetragonal distortion, is fundamental in FeGa alloys, and therefore, it can be used to tailor the magnetic anisotropy by means of the local order. In addition, the growth power determines the coercivity of the layers through the medium range order.

## CONCLUSIONS

We have investigated the influence of the growth power on the magnetic properties of Ga-rich  $\text{Fe}_{100-x}\text{Ga}_x$  ( $x$  ca. 29) thin films deposited by sputtering in the ballistic regime in oblique incidence. The experimental results show that the variation of the growth power has a small effect on the Ga content being possible to correlate the power with the structural and magnetic properties of the layers. A decrease of the medium range order can be observed, characterized by the grain size, as the power is increased that reduces the coercivity of the films. The growth power also determines the local range order that has an impact on the in-plane magnetic anisotropy upon the enhancement of both, Ga-pairs and tetragonal distortion. This work adds clues to understand the magnetic behavior of FeGa thin films and opens the way to tune the magnetic anisotropy by means of the local range order.

## AUTHOR INFORMATION

### Corresponding Author

\*E-mail: [salascoll@esrf.fr](mailto:salascoll@esrf.fr). Phone: +33 476 88 26 35.

### ORCID

E. Salas-Colera: [0000-0001-7812-268X](https://orcid.org/0000-0001-7812-268X)

### Notes

The authors declare no competing financial interest.

## ACKNOWLEDGMENTS

This work has been financially supported through project MAT2015-66888-C3-3-R of the Spanish Ministry of Economy and Competitiveness (MINECO/FEDER) and through PR26/16-3B-2 of Santander and Universidad Complutense de Madrid. We thank “CAI Difracción de rayos-X” of UCM for the X-ray diffractometry measurements and the “Instituto de Sistemas Optoelectrónicos y Microtecnología” (ISOM) for using its facilities. We also want to thank BM25-Spline, the Spanish CRG at ESRF for providing beamtime.

## REFERENCES

- (1) Xing, Q.; Du, Y.; McQueeney, R.J.; Lograsso, T.A. Structural investigations of Fe-Ga alloys: Phase relations and magnetostrictive behavior. *Acta Mater.* **2008**, *56*, 4536–4546.
- (2) Zhang, Y. N.; Cao, J. X.; Wu, R. Q. Rigid band model for prediction of magnetostriction of iron-gallium alloys. *Appl. Phys. Lett.* **2010**, *96*, 062508.
- (3) Wang, H.; Zhang, Y. N.; Wu, R. Q.; Sun, L. Z.; Xu, D. S.; Zhang, Z. D. Understanding strong magnetostriction in  $\text{Fe}_{100-x}\text{Ga}_x$  alloys. *Sci. Rep.* **2013**, *3*, 3521.
- (4) Fin, S.; Tomasello, R.; Bisero, D.; Marangolo, M.; Sacchi, M.; Popescu, H.; Eddrief, M.; Hepburn, C.; Finocchio, G.; Carpentieri, M.; et al. In-plane rotation of magnetic stripe domains in  $\text{Fe}_{1-x}\text{Ga}_x$  thin films. *Phys. Rev. B: Condens. Matter Mater. Phys.* **2015**, *92*, 224411.

We have also addressed the study of the local range order by XANES. In general, when dealing with a complex mixture of phases like in these sputtered samples, the study can only be done qualitatively. In Figure 3b, the main peak (also defined as white line) of the XANES experimental spectra of the studied FeGa layers is presented. Similar XANES results can be found in works about Ga-rich FeGa thin films.<sup>19,20</sup> The shape and intensity of the white line is related to the proportion of the different structural phases that can be present in these samples that are: A2, B2, and  $\text{D0}_3$ . In order to highlight the differences, we present in Figure 3c, the subtracted spectra with respect to the layer deposited at the lowest growth power. For example,  $\mu(90\text{ W}) - \mu(50\text{ W})$  indicates the subtraction between the spectra for layers deposited at 90 and 50 W, respectively. The subtracted spectra exhibit one main negative peak (at around 10374 eV) followed by a maximum (at around 10400 eV), both of them indicated by arrows in Figure 3c. The negative peak has been assigned to Ga-pairs formed upon the alignment of B2 cell units, whereas the maximum at higher energies is an indication of the tetragonal distortion of the also B2 cell.<sup>20</sup> Therefore, the increase of the uniaxial in-plane magnetic anisotropy with the growth power is related to the enhancement of both, Ga-pairs and tetragonal distortion, as previous works have already pointed out.<sup>19,20</sup> Theoretical calculations have shown that rather than the direct nucleation of the  $\text{D0}_3$  phase, it appears from a cascade of congruent orderings starting from disorder A2 Ga-rich aggregates:  $\text{A2} \rightarrow \text{B2} \rightarrow \text{D0}_3$ .<sup>38</sup> The increase of the growth power can prevent the crystallization from B2 to  $\text{D0}_3$ , keeping B2 in a higher proportion respect to  $\text{D0}_3$ . The experimental results presented in this work are fundamental to shed light upon the origin of the magnetic anisotropy in FeGa thin films. Here, we have observed that the

- (5) Du, Y.; Huang, M.; Chang, S.; Schlögl, D. L.; Lograsso, T. A.; McQueeney, R. J. Relation between Ga ordering and magnetostriction of Fe-Ga alloys studied by x-ray diffuse scattering. *Phys. Rev. B: Condens. Matter Mater. Phys.* **2010**, *81*, 054432.
- (6) Laver, M.; Mudivarthi, C.; Cullen, J. R.; Flatau, A. B.; Chen, W. C.; Watson, S. M.; Wuttig, M. Magnetostriction and magnetic heterogeneities in iron-gallium. *Phys. Rev. Lett.* **2010**, *105*, 027202.
- (7) Clark, A.E.; Restorff, J.B.; Wun-Fogle, M.; Lograsso, T.A.; Schlögl, D.L. Magnetostrictive properties of body-centered cubic Fe-Ga and Fe-Ga-Al alloys. *IEEE Trans. Magn.* **2000**, *36*, 3238–3240.
- (8) Tacchi, S.; Fin, S.; Carlotti, G.; Gubbiotti, G.; Madami, M.; Barturen, M.; Marangolo, M.; Eddrief, M.; Bisero, D.; Rettori, A.; et al. Rotatable magnetic anisotropy in a Fe<sub>0.8</sub>Ga<sub>0.2</sub> thin film with stripe domains: Dynamics versus statics. *Phys. Rev. B: Condens. Matter Mater. Phys.* **2014**, *89*, 024411.
- (9) Ruffoni, M. P.; Pascarelli, S.; Grössinger, R.; Turtelli, R. S.; Bormio-Nunes, C.; Pettifer, R. F. Direct measurement of intrinsic atomic scale magnetostriction. *Phys. Rev. Lett.* **2008**, *101*, 147202.
- (10) Cullen, J.; Zhao, P.; Wuttig, M. Anisotropy of crystalline ferromagnets with defects. *J. Appl. Phys.* **2007**, *101*, 123922.
- (11) Ahmad, H.; Atulasimha, J.; Bandyopadhyay, S. Reversible strain-induced magnetization switching in FeGa nanomagnets: Pathway to a rewritable, non-volatile, non-toggle, extremely low energy straintronic memory. *Sci. Rep.* **2015**, *5*, 18264.
- (12) Barturen, M.; Milano, J.; Vásquez-Mansilla, M.; Helmann, C.; Barral, M. A.; Llois, A. M.; Eddrief, M.; Marangolo, M. Large perpendicular magnetic anisotropy in magnetostrictive Fe<sub>1-x</sub>Ga<sub>x</sub> thin films. *Phys. Rev. B: Condens. Matter Mater. Phys.* **2015**, *92*, 054418.
- (13) Ahmad, H.; Atulasimha, J.; Bandyopadhyay, S. Electric field control of magnetic states in isolated and dipole-coupled FeGa nanomagnets delineated on a PMN-PT substrate. *Nanotechnology* **2015**, *26*, 401001.
- (14) Dai, G.; Zhan, Q.; Liu, Y.; Yang, H.; Zhang, X.; Chen, B.; Li, R.-W. Mechanically tunable magnetic properties of Fe<sub>81</sub>Ga<sub>19</sub> films grown on flexible substrates. *Appl. Phys. Lett.* **2012**, *100*, 122407.
- (15) Ikeda, O.; Kainuma, R.; Ohnuma, I.; Fukamichi, K.; Ishida, K. Phase equilibria and stability of ordered b.c.c. phases in the Fe-rich portion of the Fe-Ga system. *J. Alloys Compd.* **2002**, *347*, 198.
- (16) Cao, H.; Gehring, P. M.; Devreugd, C. P.; Rodríguez-Rivera, J. A.; Li, J.; Viehland, D. Role of Nanoscale Precipitates on the Enhanced Magnetostriction of Heat-Treated Galfenol (Fe<sub>1-x</sub>Ga<sub>x</sub>). *Alloys. Phys. Rev. Lett.* **2009**, *102*, 127201.
- (17) Eddrief, M.; Zheng, Y.; Hidki, S.; Rache Salles, B.; Milano, J.; Etgens, V. H.; Marangolo, M. Metastable tetragonal structure of Fe<sub>100-x</sub>Ga<sub>x</sub> epitaxial thin films on ZnSe/GaAs(001) substrate. *Phys. Rev. B: Condens. Matter Mater. Phys.* **2011**, *84*, No. 161410(R).
- (18) Arenholz, E.; van der Laan, G.; McClure, A.; Idzerda, Y. Electronic and magnetic structure of Ga<sub>x</sub>Fe<sub>1-x</sub> thin films. *Phys. Rev. B: Condens. Matter Mater. Phys.* **2010**, *82*, No. 180405(R).
- (19) Muñoz-Noval, A.; Ordóñez-Fontes, A.; Ranchal, R. Influence of the sputtering flow regime on the structural properties and magnetic behavior of Fe-Ga thin films (Ga ~30 at.%). *Phys. Rev. B* **2016**, *93*, 214408.
- (20) Muñoz-Noval, A.; Fin, S.; Salas-Colera, E.; Bisero, D.; Ranchal, R. The role of surface to bulk ratio on the development of magnetic anisotropy in high Ga content Fe<sub>100-x</sub>Ga<sub>x</sub> thin films. *J. Alloys Compd.* **2018**, *745*, 413–420.
- (21) Pascarelli, S.; Ruffoni, M. P.; Sato Turtelli, R.; Kubel, F.; Grössinger, R. Local structure in magnetostrictive melt-spun Fe<sub>80</sub>Ga<sub>20</sub> alloys. *Phys. Rev. B: Condens. Matter Mater. Phys.* **2008**, *77*, 184406.
- (22) Ciria, M.; Proietti, M. G.; Corredor, E. C.; Coffey, D.; Begué, A.; de la Fuente, C.; Arnaud, J. I.; Ibarra, A. Crystal structure and local ordering in epitaxial Fe<sub>100-x</sub>Ga<sub>x</sub>/MgO(001) films. *J. Alloys Compd.* **2018**, *767*, 905–914.
- (23) Alvarez, R.; Garcia-Martin, J. M.; Lopez-Santos, M. C.; Rico, V.; Ferrer, F. J.; Cotrino, J.; Gonzalez-Elipe, A. R.; Palmero, A. On the Deposition Rates of Magnetron Sputtered Thin Films at Oblique Angles. *Plasma Processes Polym.* **2014**, *11*, 571–576.
- (24) Somekh, R. E. The thermalization of energetic atoms during the sputtering process. *J. Vac. Sci. Technol., A* **1984**, *2*, 1285.
- (25) Turner, G. M.; Falconer, I. S.; James, B. W.; McKenzie, D. R. Monte Carlo calculations of the properties of sputtered atoms at a substrate surface in a magnetron discharge. *J. Vac. Sci. Technol., A* **1992**, *10*, 455.
- (26) Maicas, M.; Ranchal, R.; Aroca, C.; Sánchez, P.; López, E. Magnetic properties of permalloy multilayers with alternating perpendicular anisotropies. *Eur. Phys. J. B* **2008**, *62*, 267–270.
- (27) Zhang, Y.; Zhan, Q.; Zuo, Z.; Yang, H.; Zhang, X.; Dai, G.; Liu, Y.; Yu, Y.; Wang, J.; Wang, B.; Li, R. W. Magnetization reversal in epitaxial exchange-biased IrMn/FeGa bilayers with anisotropy geometries controlled by oblique deposition. *Phys. Rev. B: Condens. Matter Mater. Phys.* **2015**, *91*, 174411.
- (28) Grier, D.; Ben-Jacob, E.; Clarke, R.; Sander, L. M. Morphology and Microstructure in Electrochemical Deposition of Zinc. *Phys. Rev. Lett.* **1986**, *56*, 1264–1267.
- (29) Thornton, J. A. High Rate Thick Film Growth. *Annu. Rev. Mater. Sci.* **1977**, *7*, 239–260.
- (30) Butera, A.; Gómez, J.; Barnard, J.A.; Weston, J.L. Magnetic anisotropy in Fe<sub>81</sub>Ga<sub>19</sub>/MgO (100) films sputtered at different powers. *Phys. B* **2006**, *384*, 262–264.
- (31) Ramírez, G.A.; Malamud, F.; Gómez, J.E.; Rodríguez, L.M.; Fregenal, D.; Butera, A.; Milano, J. Controlling the crystalline and magnetic texture in sputtered Fe<sub>0.89</sub>Ga<sub>0.11</sub> thin films: Influence of substrate and thermal treatment. *J. Magn. Magn. Mater.* **2019**, *483*, 143–151.
- (32) Ravel, B.; Newville, M. ATHENA, ARTEMIS, HEPHAESTUS: Data analysis for X-ray absorption spectroscopy using IFEFFIT. *J. Synchrotron Radiat.* **2005**, *12*, 537–541.
- (33) Ankudinov, A. L.; Ravel, B.; Rehr, J. J.; Conradson, S. D. Real-space multiple-scattering calculation and interpretation of x-ray-absorption near-edge structure. *Phys. Rev. B: Condens. Matter Mater. Phys.* **1998**, *58*, 7565.
- (34) Wyckoff, R. W. G. *Crystal structures*, 2nd ed.; Interscience Publishers: New York, NY, 1963; Vol. 1, pp 7–83.
- (35) Dunlap, R. A.; Deschamps, N. C.; Mar, R. E.; Farrell, S. P. Mössbauer effect studies of Fe<sub>100-x</sub>Ga<sub>x</sub> films prepared by combinatorial methods. *J. Phys.: Condens. Matter* **2006**, *18*, 4907.
- (36) Herzer, G. Grain size dependence of coercivity and permeability in nanocrystalline ferromagnets. *IEEE Trans. Magn.* **1990**, *26*, 1397–1402.
- (37) Kelly, S. D.; Ravel, B. EXAFS analysis with self-consistent atomic potentials. In *13th International Conference on X-ray Absorption Fine Structure*; Hedman, B., Pianetta, P., Eds.; American Institute of Physics Conference Proceedings: Melville, NY, 2007; Vol. 882, pp 135–138.
- (38) Boisse, J.; Zapolsky, H.; Khachatryan, A.G. Atomic-scale modeling of nanostructure formation in Fe-Ga alloys with giant magnetostriction: Cascade ordering and decomposition. *Acta Mater.* **2011**, *59*, 2656–2668.